Materials Chemistry and Physics 248 (2020) 122908

Contents lists available at ScienceDirect

Materials Chemistry and Physics

journal homepage: www.elsevier.com/locate/matchemphys

The effect of morphology and crystalline structure of Mo/MoO_3 layers on photocatalytic degradation of water organic pollutants

M. Szkoda [a,*], K. Trzciński [a], A.P. Nowak [a], M. Gazda [b], M. Sawczak [c], A. Lisowska-Oleksiak [a]

[a] Faculty of Chemistry, Department of Chemistry and Technology of Functional Materials, Gdańsk University of Technology, Narutowicza 11/12, 80-233, Gdansk, Poland
[b] Faculty of Applied Physics and Mathematics, Gdańsk University of Technology, Narutowicza, Gdańsk, Poland
[c] Centre of Plasma and Laser Engineering, Szewalski Institute of Fluid-Flow Machinery, Polish Academy of Sciences, Fiszera 14, Gdańsk, 80-231, Poland

HIGHLIGHTS

- Molybdenum oxide layers were formed by anodization of the Mo metallic foil.
- The photoactive material was synthesized directly on the electricity conductive substrate.
- The photoactivity of MoO_3 was tested during a photocatalytic process of MB decomposition.

GRAPHICAL ABSTRACT

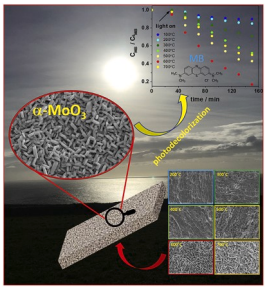

ARTICLE INFO

Keywords:
Anodization
Molybdenum trioxide
Calcination temperature
Photocatalytic properties

ABSTRACT

Molybdenum oxide layers were formed by anodization of the Mo metallic foil in a water/ethylene glycol-based electrolyte containing fluoride ions. The as-prepared, amorphous samples were annealed in air at different temperatures in a range from 100 °C to 700 °C. The crystal phase and morphology of anodized and annealed MoO_3 layers were investigated using X-ray diffraction, Raman spectroscopy, and scanning electron microscopy. The photoactivity of obtained materials was tested during a photocatalytic process of methylene blue (MB) decomposition. The increase of annealing temperature led to the production of films characterized by improved photocatalytic properties, with maximum photocatalytic efficiency observed for MoO_3 annealed at 600 °C. The studies on the use of MoO_3 as a photoelectrocatalyst for degradation of dye were performed. Furthermore, the photocatalytic activity of the MoO_3 annealed at 600 °C was investigated during a photodegradation of diclofenac acting as a model pharmaceutical compound.

1. Introduction

Ever since photocatalytic water splitting has been discovered by Fujishima and Honda in 1972 [1], researchers have been investigating numerous materials as potential photoelectrocatalysts for efficient water splitting devices. Further investigation revealed that a similar process can be applied to decompose organic compounds, for the purpose of dealing with the problem of pollution [2]. Metal oxides are among the most extensively tested types of semiconductors for this exact purpose, mainly because of their general photochemical stability, and relatively

* Corresponding author.
E-mail addresses: mariusz.szkoda1@pg.edu.pl, mariusz-szkoda@wp.pl (M. Szkoda).

https://doi.org/10.1016/j.matchemphys.2020.122908
Received 13 June 2019; Received in revised form 2 March 2020; Accepted 6 March 2020
Available online 11 March 2020

easy methods of preparation. So far many of the studies have been focused on titanium dioxide because of its nontoxicity, chemical photostability, as well as very cheap and easy synthesis methods. Unfortunately, because of the 3.2 eV bandgap, TiO_2 is active only under UV illumination, which contributes barely about 4% of the total solar energy reaching the Earth's surface [3]. Thus, finding a material with stability similar to TiO_2, exhibiting a narrower band gap and high photoactivity under visible light illumination, in order to use natural solar light for excitation is considered as a milestone in the renewable energy sector.

Molybdenum trioxide (MoO_3) is one of the several metal oxide semiconductors which is already considered as the promising candidate for replacing TiO_2. The molybdenum trioxide, as an n-type semiconductor, is one of the most intriguing transition metal oxides [4,5]. Over the past decades, MoO_3 has been widely investigated due to its properties like electrochromism [6,7], gasochromism [8], photochromism [7,9,10], photocatalytic performance [11] and capacitive behavior [12]. There are several well-developed processes and synthesis methods of MoO_3 that lead to various morphologies of this metal oxide. For most applications, MoO_3 is obtained by either the wet chemistry method approach [8], or by using molten salts synthesis [13].

In this work, we used a relatively simple electrochemical method of molybdenum metal anodization in an electrolyte containing fluoride complexing ions. The anodic oxide layers electrosynthesized in an electrolyte based on the water/ethylene glycol mixture are amorphous, non-photoactive in its pristine as received form. These layers can be transformed into crystalline phases by annealing in an air atmosphere as reported in our previous work devoted to studying photoelectrocatalytic and catalytic behavior of MoO_3 films in aqueous media [14]. It has been proven that crystal orientation has a significant influence on the catalytic activity of the MoO_3 surface. The hydroxyl radicals were identified as the most reactive oxidative species produced under solar light irradiation. However, optimization of the production conditions for the most active films is still highly desirable. In order to investigate the effect of annealing temperature on the morphology, crystalline structure, and especially photocatalytic properties of molybdenum oxide layers, the as-prepared anodic samples were annealed in air at different temperatures in the range from 100 °C to 700 °C. The proposed preparation procedure led to a deposition of photoactive layer on the conductive substrate, thus Mo/MoO_3 photoelectrodes could be used in electrochemically assisted photocatalytic degradation of organic dye, namely methylene blue (MB). Photocatalytic decolorization of MB tests were implemented as a tool for the determination of the best photocatalysts among produced films. Next, the material that exhibited the best photocatalytic properties was used for the photodecomposition of diclofenac. Diclofenac is a nonsteroidal anti-inflammatory drug of the phenylacetic acid class [15]. In general, pharmaceutical compounds belong to the most hazardous emerging pollutants in water areas [16]. These compounds can be retained into the water cycle virtually endlessly, thus, innovative solutions of pollution degradation are required, such as the advanced oxidation processes. Among them, photocatalytic and photoelectrocatalytic processes appear to be eco-friendly, giving satisfactory removal efficiencies if they are used in a proper manner. In these studies, we elaborated optimized method of MoO_3 synthesis leading to the formation of most photoactive layers. The morphology and crystal structure of those layers was controlled by applying different annealing temperatures. Obtained films of MoO_3 on Mo substrates exhibited photocatalytical activity towards degradation of methylene blue and diclofenac. It was proven, that electrochemically assisted process of pollutant degradation may significantly enhance the rate of photodecomposition.

2. Experimental

2.1. Synthesis

Molybdenum trioxide layers were prepared by electrochemical anodization of a Mo plate (Sigma Aldrich, 99.997%) in the solution with the source of fluorine ions acting as complexing agents. Prior to anodization, molybdenum sheets were ultrasonically cleaned in acetone, ethanol, and water (for 10 min in each solvent) and dried under a stream of cold air. The procedure that leads to the formation of MoO_3 was described in our previous reports [14]. The anodization process was performed in a two-electrode configuration, where a Mo plate served as an anode and a platinum rectangular mesh as a cathode (~50 cm^2). The distance between the electrodes was kept constant at 2.5 cm. The geometric area of the Mo plate was 2.5 cm^2. Anodization process took place in the electrolyte containing 0.5 M H_3PO_4 in 5%/95% vol/vol water-ethylene glycol solution with 0.1 M NH_4F. The voltage of 40 V was applied for 0.5 h and then 20 V for 1.5 h. The whole anodization process took place in a cell with the cooling jacket that kept the constant temperature at 23 °C (±1 °C) using a thermostat (Julabo F-12).

Finally, the prepared samples were cleaned using an ultrasonic bath in deionized water and thermally annealed at different temperatures between 100 and 700 °C in the air atmosphere for 2 h, with a heating rate of 2 °C min^{-1}.

The surface morphology was examined using scanning electron microscopy (SU3500, Hitachi). The UV–vis reflectance spectra of MoO_3 were measured with a dual beam UV–vis spectrophotometer (Lambda 35, PerkinElmer) equipped with a diffuse reflectance accessory. The spectra were registered in a range of 200–800 nm, with a scanning speed of 120 nm min^{-1}. Bandgap energy values were determined as the intercept of the tangent of the plot of transformation of the Kubelka–Munk function ($KM^{0.5}E_f^{0.5}$) vs. photon energy, where $KM = (1R)^2/2R$, R – reflectance. The index 0.5 is characteristic for materials characterized by indirect electron transition, including MoO_3 [13,17]. This method is commonly used for energy band gap determination of materials in a form of thick layers or grown on opaque substrates. The XPS measurements were performed using an Argus Omicron NanoTechnology X-ray photoelectron spectrometer. The photoelectrons were excited by an Mg–Kα X-ray source. The X-ray anode was operated at 15 keV and 300 W. XPS measurements were performed at room temperature under ultra-high vacuum conditions, with pressure below 1.1×10^{-8} mbar. Data analysis was performed with the CASA XPS software package using Shirley background subtraction and a least-squares Gaussian–Lorentzian curve fitting algorithm. Obtained spectra were calibrated to give binding energy of 84 eV for Au4f. Raman spectra were recorded by a confocal micro-Raman spectrometer (InVia, Renishaw) with sample excitation, by means of an argon ion laser emitting at 514 nm and operating at 5% of its total power (50 mW). Crystal structure of the obtained films were also determined by x-ray diffraction (XRD), using X-ray diffractometer (Xpert PRO-MPD, Philips) with copper Kα radiation (λ = 1.5404 Å). The photocatalytic tests were performed using 150 W solar simulator (LOT Quantum Design, LS0500/1) with AM1.5 filter and light intensity reaching the sample equals to 100 mW cm^{-2}. The photocatalytic activity of samples with a geometric area of 1 cm^2 was evaluated throughout the degradation of methylene blue (MB) aqueous solution (50 mL) with an initial concentration of 10 μM. The photoelectrocatalytic performance of Mo/MoO_3 was tested in a three-electrode cell equipped with a quartz window. The Ag/AgCl (3 M KCl) and Pt mesh act as reference and counter electrode, respectively. The potential was applied and controlled using Autolab system (PGSTAT 204). The electrochemically assisted process was performed on 75 mL of MB solution (10 μM) in 0.2 M K_2SO_4 (pH = 2). The concentration of remaining MB was controlled by absorbance measurement at λ = 662 nm wavelength (maximum of MB absorbance) using the UV–Vis spectrophotometer model UV5100 (Metash). In addition, the photocatalytic activity of the MoO_3 annealed at 600 °C was investigated during a

photodecomposition of diclofenac (in a form of sodium salt and initial concentration of 10 mg/L) in an aqueous solution. The photocatalyst was kept in the dark in 50 mL of diclofenac solution for 30 min to reach the adsorption/desorption equilibrium. The efficiency of diclofenac degradation was determined on the basis on total organic carbon (TOC) (using a Shimazu TOC analyzer model 5050 A).

3. Results and discussion

3.1. Morphology and optical properties

SEM images of the electrochemically obtained MoO_3 films before calcination, as well as calcinated are presented in Fig. 1. The film covers uniformly the entire area of the substrate, however different morphologies are observed for samples obtained at different calcination temperatures. The bare Mo foil surface before anodization is shown for comparison. The anodized film surface is characterized by the presence of an amorphous molybdenum oxide layer, with no regular, structures present on the surface. Annealing in the 100 °C–300 °C range does not create any distinctive ordered structures on the surface. One may found rather negligible differences in samples morphology at mentioned above temperature range. The first crystallites of characteristic morphology were seen for material thermally treated at 400 °C. Further temperature increase above 400 °C led to the formation of regular structures of around 1 μm length. The clear evidence of crystalline structure formation was observed after annealing at 500 °C, with the presence of small orthorhombic crystals, typical of MoO_3. Further increase in annealing temperature caused significant crystal growth, with crystal sizes of approx. 3 × 1 μm, and 30 × 10 μm for the 600 °C and 700 °C, respectively.

The morphology of the material obtained at 700 °C is less ordered compared to the material obtained at 500 °C and 600 °C.

The UV–Vis spectra of investigated samples were measured in order to study their optical properties (Fig. 2). Spectra of the samples annealed at low temperatures (100–200 °C) exhibit maximum absorption at the UV range, but there is no clear absorption edge. The shape of the absorption spectra is closely related to the crystallinity of the samples. Higher temperatures of annealing and the formation of the crystal phase cause that the spectra show the sharp absorption edge associated with the presence of a energy gap, which can be estimated at ~2.8 eV (~440 nm) for sample annealed at 400, 500 °C. The value is in an good agreement with previously reported data [13,17]. Examples of Kubelki-Munk functions are shown in Fig. S1 in supplementary information. Interestingly, the UV–Vis spectrum of the sample annealed at 600 °C is characterized by high absorption even at higher wavelengths. The extended absorption is consistent with the changes of sample color from gray to black (photograph is shown in the inset of Fig. 2c) for this material. It is beneficial for the materials that we want to use in the photocatalytical applications. The observed effect may be related to the specific morphology of obtained MoO_3.

However, molybdenum substrate can act as a reducer and the thermal reduction of MoO_3 near metallic substrate should be also taken into account. Thus, XPS measurements have been performed in order to investigate surface composition of the investigated samples. As it is shown in Fig. S2, sample annealed at 600 °C except of Mo(VI) characteristic for MoO_3 contains reduced Mo centers responsible for the absorption at visible range of radiation. The similar effect has been already reported for thermally treated TiO_2 (black TiO_2) and was assigned to the presence of Ti3+ and oxygen vacancies with trapped electrons [18]. The effect of Mo(VI) reduction is not detected using surface sensitive XPS

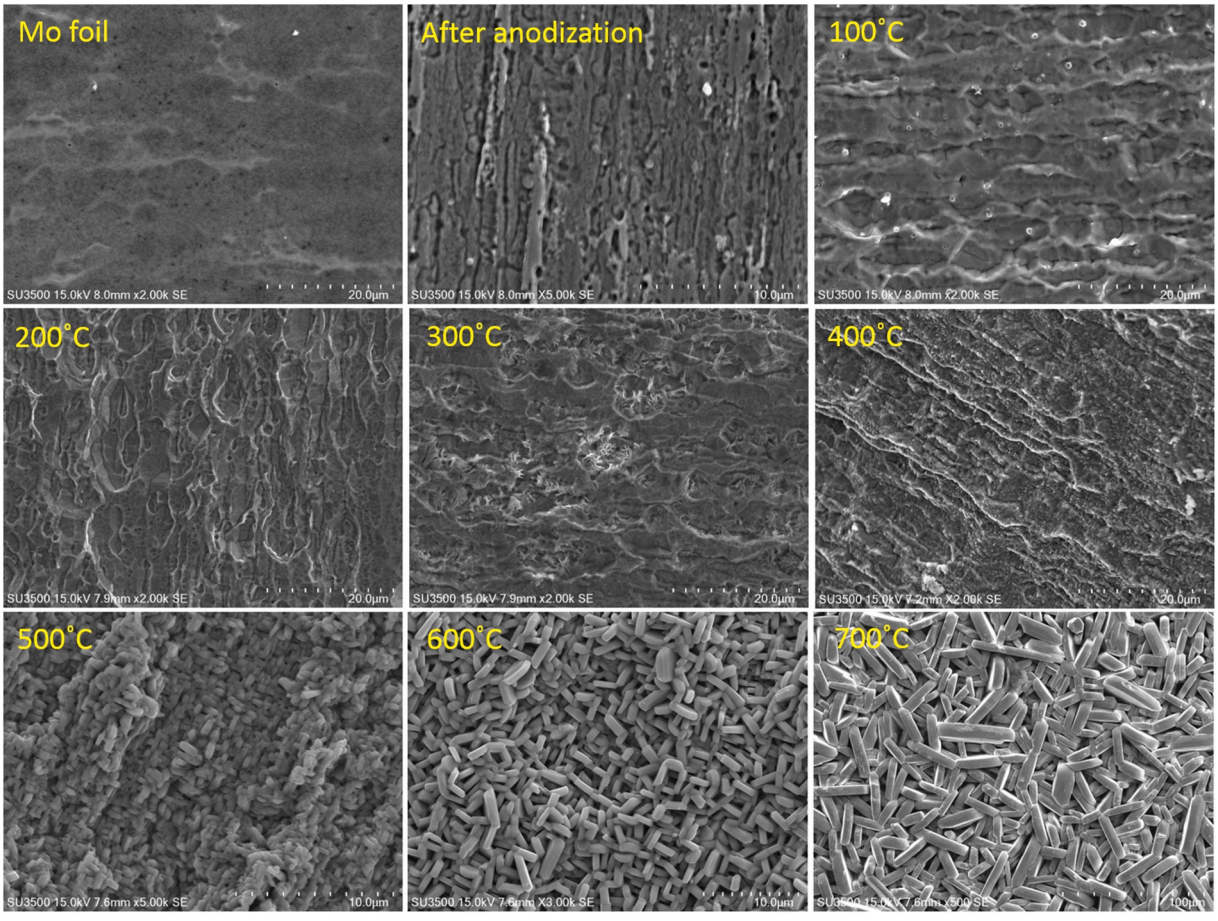

Fig. 1. The SEM images of Mo foil, MoO_3 surface after anodization, and annealed in the 100 °C–700 °C range.

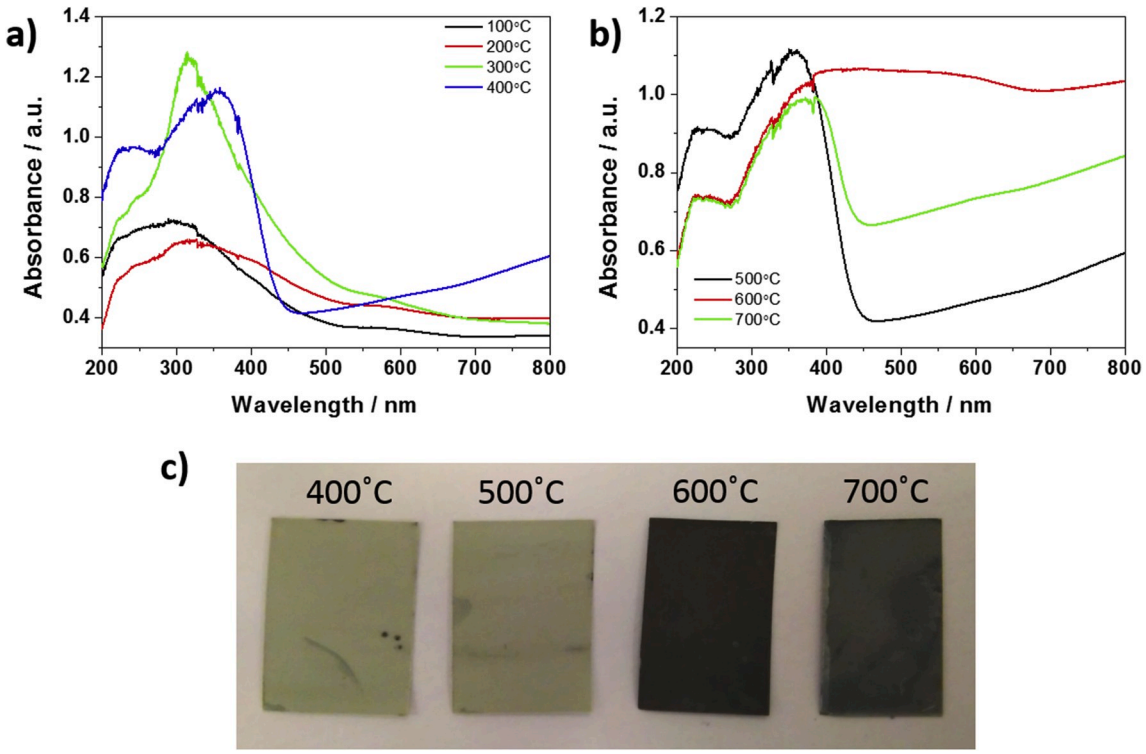

Fig. 2. a) and b) Absorbance spectra of obtained materials. c) Photograph of MoO_3 samples annealed in 400–700 °C temperature range.

spectrum of the sample annealed at 700 °C. However, the enhanced absorption at lower energies and shift of the energy bang gap towards higher wavelengths is clearly observed, proving that thermal reduction occurs at high temperatures.

3.2. Structure

As it is shown in the Raman spectra (Fig. 3), the thermal treatment at 500 °C or higher is crucial to obtain the molybdenum oxide of the ordered crystal structure (α-MoO_3). The Raman spectra showed that temperatures up to 300 °C were insufficient for MoO_3 to reach the phase transition from amorphous to the crystal structure. However, at 300 °C, a low intensity band at around 815 cm^{-1} can be observed. Also, the sample annealed at 400 °C exhibited only short-range ordering seen as the set of bands on the Raman spectrum. The crystalline MoO_3 was obtained at temperatures higher than 400 °C and can be distinguished by the main band seen at 818 cm^{-1} caused by doubly coordinated

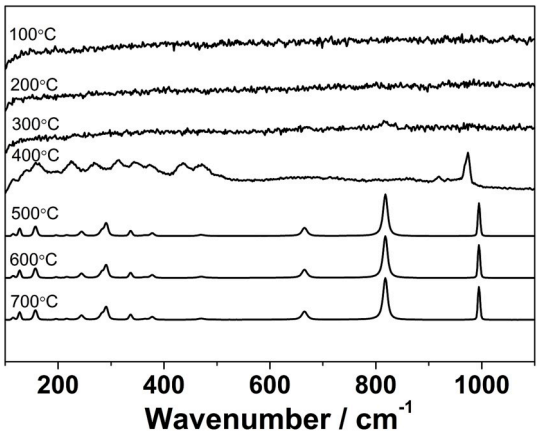

Fig. 3. Raman spectra of MoO_3 samples annealed in 100–700 °C temperature range.

bridging oxygen (Mo_2 – O) stretching mode [13]. Another maximum, detected at 996 cm^{-1}, is attributed to terminal oxygen stretching vibrations (Mo = O) [9]. The third peak at 665 cm^{-1} is assigned to triply coordinated bridging oxygen (Mo_3 - O) stretching mode of α-MoO_3 [9]. The bands that are seen below 400 cm^{-1} might be attributed to various bending vibrations and lattice modes of α-MoO_3.

To examine the long-range order, XRD analysis was conducted for the obtained samples (Fig. 4). For samples calcinated at temperatures below 300 °C, XRD patterns did not show any reflections confirming the presence of crystalline structures of MoO_3. The only signal recorded at 58° was attributed to the metallic molybdenum substrate. In the pattern of the sample annealed at 300 °C a small reflection at 27.5° is present (Fig. 4b). This reflection corresponds to the (021) plane of the orthorhombic MoO_3. This indicates that the first crystallites of molybdenum oxide form at this temperature. These results agree with conclusions obtained from the interpretation of Raman spectra for the temperature range from 100 to 400 °C.

Clearly seen reflections showing the formation of crystalline structures were identified for the sample calcinated at 400 °C. The main reflections at 23.3°, 45.7°, and 46.3° are characteristic of the (110), (200), and (210) planes of the orthorhombic MoO_3, respectively. In the pattern of polycrystalline MoO_3, shown in the reference pattern of MoO_3 (Crystallography open database - COD 9014987), the (021) reflections should have the highest intensity, whereas these of the (110), (200), and (210) planes should be much lower. The high intensity of the (110), (200), and (210) reflections suggests anisotropic growth of crystals on the pre-anodized Mo foil. It is consistent with previously reported data [14,15]. The anisotropy increases with increasing annealing temperature and is the highest in the α-MoO_3 thin film obtained at 600 °C. Such an effect was already reported in [14,19], and is crucial in terms of photocatalytic activity. In the XRD pattern of the sample annealed at 700 °C, apart from the reflections characteristic of the orthorhombic MoO_3, other reflections are present. They correspond to the monoclinic β-MoO_3 [20]. Forming of the metastable monoclinic polymorph may be caused by strain induced by solid-state crystallization. Raman spectra of the sample annealed at 700 °C do not differ from these obtained at 500

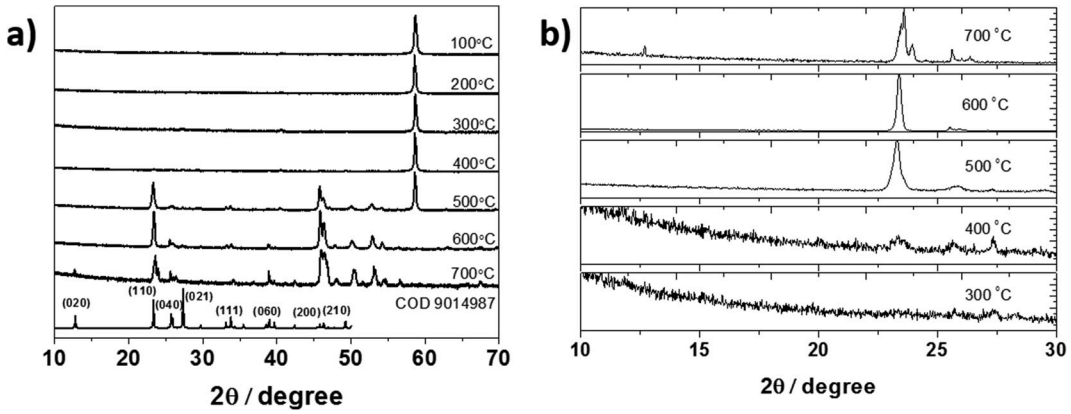

Fig. 4. XRD patterns of MoO_3 samples annealed at different temperatures.

°C and 600 °C, because Raman spectroscopy is a surface sensitive technique that depends on scattering which gives vibrational changes due to defects/vacancies present on the surface of the material. It should be also noted that the reflection seen at 58°, which corresponds to the Mo metallic support, is very high in the case of the samples annealed at temperature between 100 °C and 500 °C, whereas for the samples annealed at 600 °C and 700 °C it can hardly be seen. It is related to the formation of a thicker layer of MoO_3 in the case of the samples annealed at higher temperatures.

3.3. Photocatalytic performance

3.3.1. Photocatalytic properties

The photocatalytic performance of obtained samples was tested as a function of dye decolorization rate, with methylene blue (MB) functioning as a model organic pollutant. For comparison, a blank experiment carried out without photocatalyst is also given and photodecomposition in this case did not exceed 9%. Before illumination, every sample was kept in the dark for 30 min to achieve an adsorption/desorption equilibrium of MB on the film surface and then illuminated for 2 h. The decolorization rate of MB under simulated solar light represented as the ratio of MB concentration in the solution compared to the base concentration at the specific time, for all samples is presented in Fig. 5a.

Although for MoO_3 films calcinated in the 100 °C–200 °C temperature range a change in the concentration ratio of MB is observed, it is attributed to MB photodecomposition with no photocatalytic processes taking place on MoO_3 surface, as crystalline MoO_3 was not formed (see Fig. 5a). Further increase of annealing temperature produced films with improved photocatalytic properties, with maximum photocatalytic efficiency observed for MoO_3 annealed at 600 °C. After 2 h of illumination, MB degradation reached 83%. For the sample thermally treated at 700 °C a lower MB decomposition rate was recorded, with only 50% efficiency of MB degradation after full-time exposure. The higher efficiency of MB degradation for the sample annealed at 600 °C, in comparison with the sample prepared at 700 °C, might result from the different morphology and grain crystal sizes of the samples. Moreover, the material obtained at the temperature of 700 °C is characterized by much higher crystallites, which affects decreased photocatalytic efficiency. As it was shown in the XRD patterns in Fig. 4, the (110) crystallographic facet of α-MoO_3 (for 600 °C) is more exposed than in the case of molybdenum oxide of (020) face. The correlation between exposed crystal plane and charge stored during illumination was already reported for MoO_3 [19], as well as for TiO_2 and other semiconductor photocatalysts [21]. In addition, it has been already proven that highly oriented (110) MoO_3 crystalline planes are characterized by faster charging coefficient, as well as improved efficiency in harvesting and storing solar energy. This leads in the enhancement of high photocatalytic efficiency of the material in illuminated conditions, as well as in the dark [21]. Therefore, one may suggest that the formation of chemical species, responsible for photodegradation occurs at a specific crystal facet [110] of the photocatalyst. Moreover, the presence of reduced Mo centers also improves photocatalytic and optic properties of the sample. The very similar effect has been already reported for thermally treated TiO_2 (black TiO_2) and was assigned to the presence of Ti^{3+} and oxygen vacancies with trapped electrons [18]. In the case of reduced Mo, there are the oxygen vacancies are responsible for the increased visible-and infrared-light absorption as they can introduce localized states into the bandgap. At the same time, the oxygen vacancies act as traps for reducing the recombination of electrons and holes and significantly improve the e–h separation efficiency, thus greatly enhancing the photocatalytic activity.

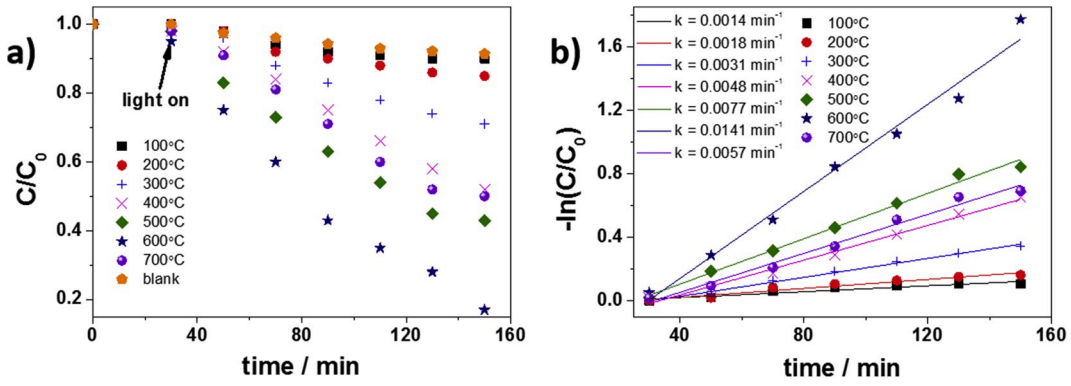

Fig. 5. a) Photocatalytic performance of the obtained samples under UV–Vis illumination. b) The kinetics of MB degradation in the presence of obtained materials used as photocatalysts.

Obtained results were compared to the previous literature reports on titania based photocatalysts (the most commonly used photocatalyst) illuminated with visible or simulated solar light. After 1 h of irradiation, the efficiency of MB photodegradation reached: 36% (boron-fluorine doped TiO_2 [22]), 34% (TiO_2/CdSe heterostructure [23]), 35% (Fe-doped TiO_2 [24]), 39% (graphene-TiO_2 [25]), 46% (C-doped TiO_2 [26]). In our report, the degradation efficiency after 1 h reached 58%. Thus, results are comparable with previously reported values for modified and improved photocatalysts which are based on TiO_2, but our material is unmodified.

In general, the decomposition reaction can be treated as a pseudo-first order reaction, where the reactions rate constants k can be calculated from the slope for lnc = f(t) function. Fig. 5b shows the rate of constant values of MB degradation in the presence of obtained materials that were used as photocatalyst. The calculated rate constant values for the different samples ranged from k = 0.0014 min^{-1} for the 100 °C annealed sample, up to 0.0141 min^{-1} for the 600 °C one. Assuming a constant decomposition rate, an arbitrary 95% degradation threshold should be reached after approximately 385 min for the MoO_3 sample annealed at 500 °C, with the reaction constant k = 0.0077 min^{-1}, and approx. 212 min for the 600 °C one (k = 0.0141 min^{-1}).

For the material characterized by the highest photoactivity (MoO_3 600 °C), 4 subsequent cycles of methylene blue photodecomposition have been performed. The photocatalyst has been regenerated through the calcination process (600 °C, 10 min) before it was applied in the next cycle photocatalytic test. The efficiency of degradation was kept almost constant in each reaction cycle. The data presented in Fig. 6 showed only a slight decrease of the photocatalytic degradation (about 5%) in four subsequent cycles. Thus, the obtained results suggest that the degradation efficiency was kept almost constant in each reaction cycle during irradiation, and consequently, the photocatalysts could be reused.

3.3.2. *Photoelectrocatalytic properties*

The photoactive material was synthesized directly on the electricity conductive substrate. It allows to test the effect of applied potential on the photocatalytic performance of studied material. The electrochemically-assisted photocatalytic measurements were performed for the Mo/MoO_3 annealed at 600 °C. Photoelectrocatalytic measurements were performed at selected potentials within the range between 0.2 V and 0.6 V *vs.* Ag/AgCl/3 M KCl in the aqueous electrolyte contains 10 μM MB. Additionally, the photoelectrochemical tests in the electrolyte without the addition of MB have been performed, The chronoamperometry curves recorded under intermittent illumination are shown in Fig. S3. The anodic photocurrent of water oxidation was recorded proving that MoO_3 films can act as potential photoanodes for water splitting. However, the generation of the photocurrent is limited due to the photointercalation effect as it was reported previously [27]. It is known that the Mo substrate is not stable at higher anodic potential due to the Mo oxidation reaction. Electrodes were initially kept in the dark for 30 min to achieve steady state conditions followed by periodical exposure to simulated sunlight. According to the results shown in Fig. 7a, the maximum value of the degradation is reached at potential *E* = +0.6 V and equals 100% after the 80 min lighting time. Thus, electrochemical assisted route significantly affects the efficiency of dye degradation. The relatively simple method is possible to utilized only for photoactive materials deposited on the conductive substrates. The possible reason of the observed enhancement may be related to the total effect for photocatalytic and electrocatalytic ways of methylene blue degradation [28]. However, one should take into account that MoO_3 is n-type semiconductor, and applying potential higher than flat band potential leads to the formation of depletion layer on the photocatalyst near the electrode/electrolyte interface. The gradient of potential through the photocatalyst film, schematically marked as band bending, facilitates electron/hole pairs separation and hinders the adverse recombination processes. As it is presented in linear voltammetry curves (see Fig. S4 in supplementary information), the higher potential applied, the higher photocurrent of MB photelectrooxidation (the difference between dark current and that recorded during illumination) is recorded. Since the Mo/MoO_3 acts here as a photoanode, it is very likely that MB is photoelectrooxidized directly on the surface and/or simultaneous radiation and applied potential leads to enhanced generation of hydroxyl radicals. The corresponding reaction rate constants are 0.0031, 0.0137, 0.185, 0.0252 and 0,0140 min^{-1} for external applied potential at 0.6 (light off), 0.2, 0.4, 0.6 V and rest potential, respectively (Fig. 7b). The used of electrochemically-assisted photocatalytic process exhibit more excellent decolorization efficiency than classical photocatalysis.

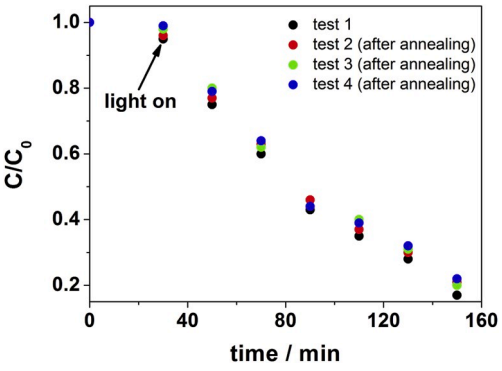

Fig. 6. Subsequent tests of MB photodecolorization in the presence of MoO_3 (600 °C) as a photocatalyst.

3.3.3. *Photodegradation of diclofenac*

The photocatalytic activity of the MoO_3 annealed at 600 °C was also investigated during photodegradation of diclofenac that served as a model pharmaceutical compound. The mineralization of the pharmaceutical was followed by total organic carbon (TOC) disappearance. The obtained results are shown in Fig. 8. A control experiment carried out without a photocatalyst sample was performed for comparison and gave a very limited decrease of TOC (from 10 to 9.88 mg/L). The photocatalytic process of diclofenac degradation in the presence of MoO_3 photocatalyst under simulated solar illumination led to the oxidation of pollution to CO_2 with 25% efficiency.

4. Conclusions

In this work optimization procedure, leading to the construction of the re-useable photocatalyst in a form of thin layers, deposited on solid metal Mo support is presented. The Mo/MoO_3 is used as a photocatalyst active under visible light illumination. Here we showed that depending on calcination temperature, obtained MoO_3 films have different crystalline structures and morphologies, which strongly affects photocatalytic activity. Clearly seen reflections showing the formation of crystalline structures were identified for the sample calcinated at 400 °C. The main reflections at 23.3°, 45.7°, and 46.3° are characteristic of the (110), (200), and (210) planes of the orthorhombic MoO_3, respectively. Pure α-MoO_3 with oriented crystal structure was obtained after annealing at 500 °C and 600 °C, which was confirmed by XRD analysis and Raman spectroscopy independently. Thermal treatment of the sample at 700 °C showed more randomly arranged crystallites and a loss of specific orientation exposing (110) facet of α-MoO_3. In the XRD pattern of the sample annealed at 700 °C, apart from the reflections characteristic of the orthorhombic MoO_3, other reflections are present. They correspond to the monoclinic β-MoO_3. The crystallites size increased 15 times. Moreover, such a change of crystallographic structure and morphology contributed to the s significant diminution of the photocatalytic performance of the sample annealed at 700 °C.

MB decomposition constant rates were calculated to evaluate the photocatalytic properties of the material. With an annealing temperature increase, an increase of MB decomposition constant rate was

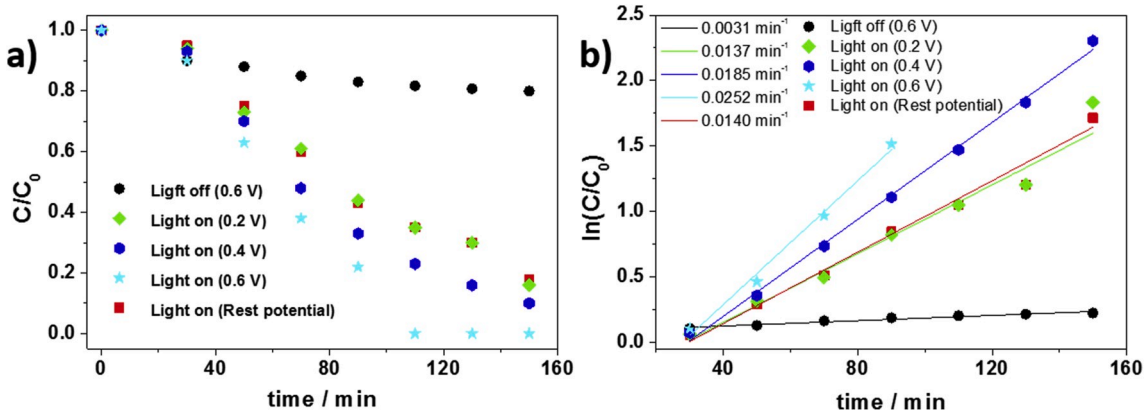

Fig. 7. a) The electrochemically-assisted photocatalytic performance of the selected samples under UV–vis illumination. b) The kinetics of MB photoelectrodegratation in the presence of Mo/MoO_3 (600 °C) used as photocatalysts.

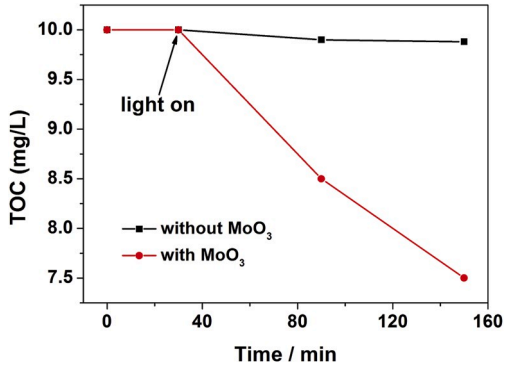

Fig. 8. The efficiency of diclofenac photodegradation measured as disappearance of total organic carbon.

observed, with the maximum decomposition rate equals to 0.0141 min^{-1} for the sample calcinated at 600 °C. Further temperature increase caused the decrease of decomposition constant rate to 0.0057 min^{-1} due to the re-crystallization process and loss of anisotropy. The photocatalyst deposited onto the conductive substrate may be used as a catalyst in electrochemically-assisted photodecomposition of organic pollutants. The significant enhancement of rate constant was achieved, with 0.0252 min^{-1} for 0.6 V and was higher around 1.8 times compared to the value without electrochemically-assisted. MoO_3 can be also an effective photocatalyst for pharmaceutical removal from aqueous solutions (on the example of diclofenac).

Summarizing, Mo/MoO_3 (600 °C) prepared by electrochemical anodization and properly annealed is promising material characterized by a high organic compound photodecomposition rate and could become an alternative option for practical applications.

Declaration of competing interest

The authors declare that they have no known competing financial interests or personal relationships that could have appeared to influence the work reported in this paper.

CRediT authorship contribution statement

M. Szkoda: Conceptualization, Investigation, Writing - original draft, Writing - review & editing. **K. Trzciński:** Validation, Writing - original draft, Writing - review & editing. **A.P. Nowak:** Investigation. **M. Gazda:** Investigation. **M. Sawczak:** Investigation, Methodology, Visualization. **A. Lisowska-Oleksiak:** Supervision.

Acknowledgment

MS acknowledges the National Science Centre of Poland, NCN, for financial support under contract 2016/23/N/ST5/02071. M.S. is supported by the Foundation for Polish Science. Authors would like to acknowledge PhD Maciej Klein for SEM images and Gabor Fierka for help in interpreting the results.

Appendix A. Supplementary data

Supplementary data to this article can be found online at https://doi.org/10.1016/j.matchemphys.2020.122908.

References

[1] A. Fujishima, K. Honda, Electrochemical photolysis of water at a semiconductor electrode, Nature 238 (1972) 37–38.
[2] S.N. Frank, A.J. Bard, S.N. Frank, A.J. Bard, Heterogeneous photocatalytic oxidation of cyanide and sulfite in aqueous solutions at semiconductor, Powders 81 (1977) 1484–1488, https://doi.org/10.1021/j100530a011.
[3] A. Heller, Hydrogen-evolving solar cells, Science 379 (1982) 1141–1148, https://doi.org/10.1126/science.223.4641.1141.
[4] S. Santhosh, M. Mathankumar, S. Selva Chandrasekaran, A.K. Nanda Kumar, P. Murugan, B. Subramanian, Effect of ablation rate on the microstructure and electrochromic properties of pulsed-laser-deposited molybdenum oxide thin films, Langmuir 33 (2017) 19–33, https://doi.org/10.1021/acs.langmuir.6b02940.
[5] P.R. Huang, Y. He, C. Cao, Z.H. Lu, Impact of lattice distortion and electron doping on α-MoO_3electronic structure, Sci. Rep. 4 (2014) 1–7, https://doi.org/10.1038/srep07131.
[6] T.M. McEvoy, K.J. Stevenson, J.T. Hupp, X. Dang, Electrochemical preparation of molybdenum trioxide thin films: effect of sintering on electrochromic and electro insertion properties, Langmuir 19 (2003) 4316–4326, https://doi.org/10.1021/la027020u.
[7] J.N. Yao, B.H. Loo, A. Fujishima, A study of the photochromic and electrochromic properties of MoO_3 thin films, Phys. Chem. 94 (1990) 13–17, https://doi.org/10.1002/bbpc.19900940104.
[8] I.A. de Castro, R.S. Datta, J.Z. Ou, A. Castellanos-Gomez, S. Sriram, T. Daeneke, K. Kalantar-Zadeh, Molybdenum oxides - from fundamentals to functionality, Adv. Mater. (2017) 1701619, https://doi.org/10.1002/adma.201701619, 1701619.
[9] K. Ajito, L.A. Nagahara, D.A. Tryk, K. Hashimoto, A. Fujishima, Study of the photochromic properties of amorphous MoO_3 films using Raman microscopy, J. Phys. Chem. 99 (1995) 16383–16388, https://doi.org/10.1021/j100044a028.
[10] M. Szkoda, K. Trzciński, M. Klein, K. Siuzdak, A. Lisowska-Oleksiak, The influence of photointercalaction and photochromism effects on the photocatalytic properties of electrochemically obtained maze-like MoO_3 microstructures, Separ. Purif. Technol. 197 (2018) 382–387, https://doi.org/10.1016/j.seppur.2018.01.033.
[11] A. Chithambararaj, N.S. Sanjini, S. Velmathi, a C. Bose, Preparation of h-MoO_3 and α-MoO_3 nanocrystals: comparative study on photocatalytic degradation of methylene blue under visible light irradiation, Phys. Chem. Chem. Phys. 15 (2013) 14761–14769, https://doi.org/10.1039/c3cp51796a.
[12] H. Zhang, L. Gao, Y. Gong, Exfoliated MoO_3 nanosheets for high-capacity lithium storage, Electrochem. Commun. 52 (2015) 67–70, https://doi.org/10.1016/j.elecom.2015.01.014.
[13] S. Alizadeh, S.a. Hassanzadeh-Tabrizi, MoO3 fibers and belts: molten salt synthesis, characterization and optical properties, Ceram. Int. 41 (2015) 10839–10843, https://doi.org/10.1016/j.ceramint.2015.05.024.

[14] M. Szkoda, K. Trzciński, K. Siuzdak, A. Lisowska-Oleksiak, Photocatalytical properties of maze-like MoO_3 microstructures prepared by anodization of Mo plate, Electrochim. Acta 228 (2017) 139–145, https://doi.org/10.1016/j.electacta.2017.01.064.
[15] N. Vieno, M. Sillanpää, Fate of diclofenac in municipal wastewater treatment plant — a review, Environ. Int. 69 (2014) 28–39, https://doi.org/10.1016/j.envint.2014.03.021.
[16] J.C.G. Sousa, A.R. Ribeiro, M.O. Barbosa, M.F.R. Pereira, A.M.T. Silva, A review on environmental monitoring of water organic pollutants identified by EU guidelines, J. Hazard Mater. 344 (2018) 146–162, https://doi.org/10.1016/j.jhazmat.2017.09.058.
[17] X. Chen, W. Lei, D. Liu, J. Hao, Q. Cui, G. Zou, Synthesis and characterization of hexagonal and truncated hexagonal shaped MoO_3 nanoplates, J. Phys. Chem. C 113 (2009) 21582–21585, https://doi.org/10.1021/jp908155m.
[18] S. Chen, Y. Xiao, Y. Wang, A facile approach to prepare black TiO_2 with oxygen vacancy for enhancing photocatalytic activity, Nanomaterials 8 (2018) 245, https://doi.org/10.3390/nano8040245.
[19] S.N. Lou, N. Yap, J. Scott, R. Amal, Y.H. Ng, Influence of MoO_3(110) crystalline plane on its self-charging photoelectrochemical properties, Sci. Rep. 4 (2014) 7428, https://doi.org/10.1038/srep07428.
[20] A. Stoyanova, R. Iordanova, M. Mancheva, Y. Dimitriev, Synthesis and structural characterization of MoO_3 phases obtained from molybdic acid by addition of HNO_3 and H_2O_2, J. Optoelectron. Adv. Mater. 11 (2009) 1127–1131.
[21] X. Han, Q. Kuang, M. Jin, Z. Xie, L. Zheng, Synthesis of titania nanosheets with a high percentage of exposed (001) facets and related photocatalytic properties, J. Am. Chem. Soc. 131 (2009) 3152–3153, https://doi.org/10.1021/ja8092373.
[22] H. Li, J. Xing, Z. Xia, J. Chen, Preparation of extremely smooth and boron-fluorine co-doped TiO_2 nanotube arrays with enhanced photoelectrochemical and photocatalytic performance, Electrochim. Acta 139 (2014) 331–336, https://doi.org/10.1016/j.electacta.2014.06.172.
[23] C. Lu, L. Zhang, Y. Zhang, S. Liu, Electrodeposition of TiO_2/CdSe heterostructure films and photocatalytic degradation of methylene blue, Mater. Lett. 185 (2016) 342–345, https://doi.org/10.1016/j.matlet.2016.09.017.
[24] C. Fàbrega, T. Andreu, A. Cabot, J.R. Morante, Location and catalytic role of iron species in TiO_2:Fe photocatalysts: an EPR study, J. Photochem. Photobiol. Chem. 211 (2010) 170–175, https://doi.org/10.1016/j.jphotochem.2010.03.003.
[25] D. Zhao, G. Sheng, C. Chen, X. Wang, Enhanced photocatalytic degradation of methylene blue under visible irradiation on graphene@TiO_2 dyade structure, Appl. Catal. B Environ. 111–112 (2012) 303–308, https://doi.org/10.1016/j.apcatb.2011.10.012.
[26] J. Matos, A. García, L. Zhao, M.M. Titirici, Solvothermal carbon-doped TiO_2 photocatalyst for the enhanced methylene blue degradation under visible light, Appl. Catal. Gen. 390 (2010) 175–182, https://doi.org/10.1016/j.apcata.2010.10.009.
[27] M. Szkoda, K. Trzciński, M. Łapiński, A. Lisowska-Oleksiak, Photoinduced K+ intercalation into MoO_3/FTO photoanode — the impact on the photoelectrochemical performance, Electrocatalysis (2019), https://doi.org/10.1007/s12678-019-00561-2.
[28] J. Li, L. Zheng, L. Li, Y. Xian, L. Jin, Fabrication of TiO_2/Ti electrode by laser-assisted anodic oxidation and its application on photoelectrocatalytic degradation of methylene blue, J. Hazard Mater. 139 (2007) 72–78, https://doi.org/10.1016/j.jhazmat.2006.06.003.